*Coupled Systems Mechanics, Vol. 1, No. 1 (2012) 19-37*
DOI: http://dx.doi.org/10.12989/csm.2012.1.1.019


# FEM-BEM iterative coupling procedures to analyze interacting wave propagation models: fluid-fluid, solid-solid and fluid-solid analyses

Delfim Soares Jr.*

*Structural Engineering Department, Federal University of Juiz de Fora, CEP 36036-330 Juiz de Fora, MG, Brazil*

*(Received December 20, 2011, Revised February 10, 2012, Accepted February 13, 2012)*

**Abstract.** In this work, the iterative coupling of finite element and boundary element methods for the investigation of coupled fluid-fluid, solid-solid and fluid-solid wave propagation models is reviewed. In order to perform the coupling of the two numerical methods, a successive renewal of the variables on the common interface between the two sub-domains is performed through an iterative procedure until convergence is achieved. In the case of local nonlinearities within the finite element sub-domain, it is straightforward to perform the iterative coupling together with the iterations needed to solve the nonlinear system. In particular, a more efficient and stable performance of the coupling procedure is achieved by a special formulation that allows to use different time steps in each sub-domain. Optimized relaxation parameters are also considered in the analyses, in order to speed up and/or to ensure the convergence of the iterative process.

**Keywords:** wave propagation; iterative coupling; finite element method; boundary element method; multi-domain decomposition; different time-steps; nonlinear calculations

## 1. Introduction

The numerical simulation of arbitrarily shaped continuous bodies - solids and/or fluids - subjected to harmonic or transient loads remains, despite much effort and progress over the last decades, a challenging area of research. In most cases, discrete techniques, such as the Finite Element Method (FEM) and the Boundary Element Method (BEM) have been employed and continuously further developed with respect to accuracy and efficiency. Both methodologies can be formulated in the time domain or in the frequency domain, and each approach has relative benefits and limitations. The Finite Element Method, for instance, is well suited for inhomogeneous and anisotropic materials as well as for dealing with the nonlinear behavior of a body. For systems with infinite extension and regions of high gradient/stress concentration, however, the use of the Boundary Element Method is more advantageous. Further details are given, e.g., by Hughes (1987) or Bathe (1996) for the FEM and by Becker (1992) or Dominguez (1993) in the case of the BEM.

In fact, it did not take long until some researchers started to combine the FEM and the BEM in order to profit from their respective advantages by trying to evade their disadvantages. Up to now,

* Corresponding author, Professor, E-mail: delfim.soares@ufjf.edu.br

quite a few publications concentrate on such coupling approaches. Many details are given, e.g., by Zienkiewicz *et al*. (1977,1979), who were among the first suggesting a "*mariage à la mode - the best of two worlds"*, by von Estorff and Prabucki (1990), von Estorff and Antes (1991), Belytschko and Lu (1994), Yu *et al*. (2001) etc.. A rather complete overview is provided by Beskos (1987, 1996, 2003). It should be mentioned, that in most cases the BEM has been used to model those parts of the investigated bodies that are of semi-infinite extension, while finite parts were represented with the FEM.

The FEM-BEM coupling in the time domain has also been successfully used to take into account nonlinear effects. Thus Pavlatos and Beskos (1994) as well as Yazdchi *et al*. (1999), for instance, modeled an inelastic structure and the surrounding soil part expected to become inelastic by the FEM and the remaining soil assumed to behave linearly by means of the BEM. A Similar approach has been used in some publications by von Estorff and Firuziaan (2000), and Firuziaan and von Estorff (2002). The coupling of an inelastic structure with a fluid domain of semi-infinite extension has been investigated by Czygan and von Estorff (2002).

Note that the coupling approaches mentioned so far were formulated in a way that, first, a coupled system of equation is established, which afterwards has to be solved using a standard direct solution scheme. Doing so, three major problems need to be taken care of:

1. Due to the coupling of the FEM system matrices with fully populated BEM influence matrices, the coupled system of equations is not banded and sparsely populated anymore. This means that for its solution the optimized solvers usually used in the FEM cannot be employed anymore, which leads to rather expensive calculations with respect to computer time.
2. If standard transient coupling approaches are employed, the duration of the time step has to be the same for each sub-domain. This sometimes leads to numerical difficulties, in particular, if strongly different materials (with different wave speeds), e.g., a solid and a fluid, need to be coupled.
3. In the case of taking into account some nonlinearity within the FEM sub-region, the rather big coupled system of equations needs to be solved in each step of the iterative process, i.e., a few times within each time step. This is very computer time consuming.

In view of the first aspect, Elleithy *et al*. (2001) got the idea of coupling the FEM and the BEM iteratively. However, they were interested only in the solution of elastostatic problems. Later, Elleithy *et al*. (2002, 2009) applied the iterative FEM-BEM coupling procedure to solve the Laplace equation as well as some other more complex static models (elastoplasticity). Other authors also implemented iterative FEM-BEM coupling procedures to analyze permanent/static mechanical problems (e.g., Lin 1996, Bo *et al*. 2006 etc.), highlighting the benefits of the iterative procedure. Considering wave propagation analyses, Soares *et al*. (2004, 2005b) firstly applied the iterative formulation to analyze coupled dynamic and/or acoustic models. Later on, the iterative FEM-BEM coupling methodology was improved (Soares, 2008b, 2009a,c), rendering more stable and efficient techniques. The procedure was also applied to the coupling of different numerical methods, rather than the FEM and the BEM, as well as for different physical applications, rather than those considered by computational mechanics, expanding the generality and versatility of the technique (Soares *et al*. 2005a, 2006, 2008a,c, 2009b, 2011, 2012, von Estorff and Hagen 2005, Warszawski *et al*. 2008).

In the present paper, the iterative FEM-BEM coupling scheme for the investigation of wave propagation models is reviewed. It turns out to be very efficient with respect not only to the first but also to the second and third aspects mentioned above. The FEM and the BEM parts are based on usual formulations, as suggested, e.g., by Crisfield (1991), Belytschko *et al*. (2000), Zienkiewicz and Taylor (2002) and Mansur (1983), Dominguez (1993), von Estorff (2000), respectively. Thus,

only simple interface procedures have to be implemented if one desires to couple FEM/BEM existing codes.

The discussed iterative coupling scheme is applied to three numerical examples, namely to a fluid-fluid, solid-solid and fluid-solid system, to illustrate how the FE/BE combination can be performed, how accurate the results are, and how nonlinearities in some parts of the body can be taken into account. Boundary elements may be used for either finite or infinite parts of the body, whereas all finite element sub-regions have to be bounded domains. Adoption of optimal relaxation parameters is also discussed in the examples, illustrating their influence in the stability and efficiency of the analyses.

## 2. Governing equations

In the following sub-sections, the basic equations describing the dynamic behavior of a solid and a fluid sub-domain are briefly summarized.

### 2.1 Solid sub-domain

The momentum equilibrium equation, considering a unit volume of a continuous body, is given by

$$\sigma_{ij,j} - \rho\ddot{u}_i + \rho b_i = 0 \tag{1}$$

where $\sigma_{ij}$ is the Cauchy stress, using the usual indicial notation for Cartesian axes; $u_i$ stands for the displacement and $b_i$ for the body force distribution. Inferior commas and overdots indicate partial space ($u_{j,i} = \partial u_j / \partial x_i$) and time ($\dot{u}_i = \partial u_i / \partial t$) derivatives, respectively. $\rho$ stands for the mass density.

The constitutive law can be written incrementally as

$$d\sigma_{ij} = D_{ijkl}(d\varepsilon_{kl} - d\varepsilon^0_{kl}) + \sigma_{ik}d\omega_{kj} + \sigma_{jk}d\omega_{ki} \tag{2}$$

where the last two terms account for the Zaremba-Jaumann rotational stress changes (negligible generally in small displacement computation) and $D_{ijkl}$ is a tangential tensor defined by suitable state variables and the direction of the increment. The incremental strain ($d\varepsilon_{ij}$) and rotation ($d\omega_{ij}$) components are defined in the usual way from the displacement as

$$\begin{aligned} d\varepsilon_{ij} &= (1/2)(du_{i,j} + du_{j,i}) \\ d\omega_{ij} &= (1/2)(du_{j,i} - du_{i,j}) \end{aligned} \tag{3}$$

and $\varepsilon^0_{ij}$ refers to strains caused by external actions such as temperature changes, creep, etc.

Taking into account a linear behavior of the considered body, Eq. (1) can be written, in accordance with a linear simplified form of Eqs. (2) and (3), as

$$(c_d^2 - c_s^2)u_{j,ji} + c_s^2 u_{i,jj} - \ddot{u}_i + b_i/\rho = 0 \tag{4}$$

where $c_d$ is the dilatational wave velocity and $c_s$ is the shear wave velocity. Furthermore, boundary and initial conditions should be defined in order to completely describe the model.

### 2.2 Fluid sub-domain

If the influence of gravity on the dynamic behavior of the fluid is neglected, the hydrodynamic equilibrium equation can be obtained from the Navier-Stokes equation as

$$\hat{\rho}\dot{v}_i + p_{,i} = 0 \tag{5}$$

where $p$ stands for a potential variable, namely the hydrodynamic pressure, $v$ is the velocity of the fluid particles, and $\hat{\rho}$ the density of the fluid. Using Eq. (5) and the continuity equation

$$\hat{\rho}(v_{i,i} - a) + \dot{p}/c^2 = 0 \tag{6}$$

it is straight forward to obtain the so-called acoustic wave equation

$$p_{,ii} - \ddot{p}/c^2 + \hat{\rho}\dot{a} = 0 \tag{7}$$

which describes the irrotational small-amplitude motions of the fluid particles. In Eq. (7), $c$ is the acoustic wave velocity and $a$ gives the space and time dependence of a source density in the fluid. Once again, boundary and initial conditions need to be defined in order to complete the modeling.

## 3. Finite element modeling

In the present work, nonlinearities occurring in the solid sub-region, which is modeled with finite elements, can be taken into account. Using, for instance, Newton-Raphson iterative procedures, the governing equilibrium equations describing a nonlinear dynamic problem are given by

$$\boldsymbol{M}\ddot{\boldsymbol{U}}^n_{(k+1)} + \boldsymbol{C}\dot{\boldsymbol{U}}^n_{(k+1)} + \boldsymbol{K}_T\Delta\boldsymbol{U}_{(k+1)} = \boldsymbol{F}^n - \boldsymbol{R}^n_{(k)} \tag{8}$$

$$\boldsymbol{U}^n_{(k+1)} = \boldsymbol{U}^n_{(k)} + \Delta\boldsymbol{U}_{(k+1)} \tag{9}$$

where $\boldsymbol{M}$, $\boldsymbol{C}$, and $\boldsymbol{K}_T$ are mass, damping and nonlinear stiffness matrices, respectively. The nonlinear residual vector is represented by $\boldsymbol{F}^n - \boldsymbol{R}^n_{(k)}$ and $\Delta\boldsymbol{U}_{(k+1)}$ is the variation of the incremental displacements, calculated at each iterative step. $\boldsymbol{U}^n_{(k+1)}$, $\dot{\boldsymbol{U}}^n_{(k+1)}$ and $\ddot{\boldsymbol{U}}^n_{(k+1)}$ are the displacement, velocity and acceleration vectors, respectively, at time $t_n$ and iterative step $(k + 1)$.

Using the Newmark methodology (Newmark 1956)

$$\ddot{\boldsymbol{U}}^n = (1/(\lambda\Delta t^2))(\boldsymbol{U}^n - \boldsymbol{U}^{n-1}) - (1/(\lambda\Delta t))\dot{\boldsymbol{U}}^{n-1} - (1/(2\lambda) - 1)\ddot{\boldsymbol{U}}^{n-1} \tag{10}$$

$$\dot{\boldsymbol{U}}^n = \dot{\boldsymbol{U}}^{n-1} + (\Delta t(1-\gamma))\ddot{\boldsymbol{U}}^{n-1} + (\gamma\Delta t)\ddot{\boldsymbol{U}}^n \tag{11}$$

as well as Eqs. (8) and (9), the following effective system of equations can be achieved, which has to be solved at each iterative step of the Newton-Raphson procedure

$$\boldsymbol{A}\Delta\boldsymbol{U}_{(k+1)} = \boldsymbol{B}_{(k)} \tag{12}$$

In Eqs. (10) and (11), $\gamma \geq 0.5$ and $\lambda \geq 0.25(0.5 + \gamma)^2$ are the parameters chosen in the Newmark formulation, and $\Delta t$ is the time-step. In Eq. (12), $\boldsymbol{A}$ is the effective nonlinear dynamic matrix and $\boldsymbol{B}_{(k)}$ is the effective residual vector. Further details on the implementation of the Newmark/Newton-Raphson algorithm can be found, for instance, in Jacob and Ebecken (1994). The Eqs. (9)-(12) enable the computation of the transient FEM response at time $t_n$. They are the basis for the iterative coupling scheme with respect to the solid sub-domain, in which nonlinearities may occur.

Taking into account linear acoustic fluid models, the above formulation can be greatly simplified. In this case, the discretized governing equations can be described as

$$\boldsymbol{M}\ddot{\boldsymbol{P}}^n + \boldsymbol{C}\dot{\boldsymbol{P}}^n + \boldsymbol{K}\boldsymbol{P}^n = \boldsymbol{F}^n \tag{13}$$

where now the $\boldsymbol{M}$, $\boldsymbol{C}$ and $\boldsymbol{K}$ matrices and the $\boldsymbol{F}$ vector are related to the fluid model, and $\boldsymbol{P}$ stands for the hydrodynamic pressure nodal values. Once the Newmark method is considered, an effective system of equations, analogously to Eq. (12), can be obtained, allowing the solution of the fluid sub-domain at each time-step, by finite element procedures.

## 4. Boundary element modeling

In the present work, the boundary element method is going to be employed to deal with linear solid and acoustic fluid sub-domains. The basic equation that arises from the boundary element formulation can be written as

$$(\boldsymbol{C} + \boldsymbol{H}^1)\boldsymbol{V}_H^n = \boldsymbol{G}^1\boldsymbol{V}_G^n + \sum_{m=1}^{n-1} (\boldsymbol{G}^{n-m+1}\boldsymbol{V}_G^m - \boldsymbol{H}^{n-m+1}\boldsymbol{V}_H^m) \tag{14}$$

where $\boldsymbol{H}^n$ and $\boldsymbol{G}^n$ are the influence matrices computed at the current time step $n$ and $\boldsymbol{V}_H$ and $\boldsymbol{V}_G$ are the variables on the boundary ($\boldsymbol{C}$ is a geometric influence matrix). In the case of a solid mechanic analysis (Eq. (4)), $\boldsymbol{V}_H$ and $\boldsymbol{V}_G$ contain the boundary displacements ($\boldsymbol{U}$) and tractions ($\boldsymbol{T}$), respectively; if an acoustic fluid (Eq. (7)) is considered, $\boldsymbol{V}_H$ and $\boldsymbol{V}_G$ are the vectors in which the boundary pressures ($\boldsymbol{P}$) and fluxes ($\boldsymbol{Q}$) are assembled, respectively.

After introducing the boundary conditions in Eq. (14), the following expression is obtained

$$\hat{\boldsymbol{A}}\boldsymbol{x}^n = \hat{\boldsymbol{B}}\boldsymbol{y}^n + \boldsymbol{S}^n \tag{15}$$

where, as usual in time domain BEM, the entries of $\boldsymbol{x}^n$ are unknown variables on the boundary nodes at the discrete time $t_n$, while the entries of vector $\boldsymbol{y}^n$ are the according known nodal values. $\boldsymbol{S}^n$ is the vector related to the time convolution process of the BEM; it represents the complete history up to $t_{n-1}$. Further details on the implementation of the time-domain BEM algorithm can be found, for instance, in Dominguez (1993) and Mansur (1983).

As a last remark concerning the BE modeling, one should keep in mind that, for implementing the above numerical scheme (Eqs. (14) and (15)), an approximation in time and along the boundary is considered, following the expression below

$$V(X,t) = \sum_{j=1}^{J} \sum_{m=1}^{M} \phi^m(t)\,\eta^j(X)\,V_j^m \tag{16}$$

where $\eta^j$ is a spatial interpolation function corresponding to a boundary node $X_j$; $\phi^m$ is a time interpolation function corresponding to a discrete time $t_m$; and, finally, $V_j^m = V(X_j, t_m)$. It is important to highlight this aspect of the formulation since, in the iterative coupling algorithm, different time-steps for each sub-domain of the model is considered, and time interpolation/extrapolation procedures are carried out based on the BEM time interpolation functions $\phi^m$. It is also important to observe that usually different time interpolation functions are adopted for $\boldsymbol{V}_H$ and $\boldsymbol{V}_G$, being usually linear and piecewise constant time interpolation functions considered, respectively.

## 5. Iterative coupling procedure

In order to be able to explain the iterative coupling procedures in a more comprehensive way, a notation such as ${}^{I}_{F/B}\boldsymbol{V}^{t}_{(k)}$ is used. According to this, the variable $\boldsymbol{V}$ is on the BEM/FEM interface (${}^{I}\boldsymbol{V}$) and it is approached by the FEM or BEM sub-domain (${}_{F}\boldsymbol{V}$ or ${}_{B}\boldsymbol{V}$, respectively) at time $t$ ($\boldsymbol{V}^t$) and at the iterative step ($k$) ($\boldsymbol{V}_{(k)}$). Moreover, the functions $N(.)_i$ and $T(.)_i$ shall be introduced: at a node $i$ of the BEM/FEM interface, they lead to the normal and the tangential component of their arguments, respectively.

Considering the coupling conditions at each node $i$ of the interfaces, Eqs. (17), (18) and (19) must hold for a fluid-fluid, solid-solid and solid-fluid coupling, respectively

*Fluid-fluid coupling*

$$\begin{aligned} ({}^{I}_{F}\boldsymbol{F})_i &= -({}^{I}_{B}\tilde{\boldsymbol{Q}})_i \\ ({}^{I}_{F}\boldsymbol{P})_i &= ({}^{I}_{B}\boldsymbol{P})_i \end{aligned} \tag{17}$$

*Solid-solid coupling*

$$\begin{aligned} ({}^{I}_{F}\boldsymbol{F})_i &= -({}^{I}_{B}\tilde{\boldsymbol{T}})_i \\ ({}^{I}_{F}\boldsymbol{U})_i &= ({}^{I}_{B}\boldsymbol{U})_i \end{aligned} \tag{18}$$

*Fluid-solid coupling*

$$\begin{aligned} T({}^{I}_{F}\boldsymbol{F})_i &= 0 \\ N({}^{I}_{F}\boldsymbol{F})_i &= -({}^{I}_{B}\tilde{\boldsymbol{P}})_i \\ N({}^{I}_{F}\ddot{\boldsymbol{U}})_i &= (1/\hat{\rho})({}^{I}_{B}\boldsymbol{Q})_i \end{aligned} \tag{19}$$

where, in order to obtain consistency between the FE and the BE formulation, $\tilde{\boldsymbol{P}}$, $\tilde{\boldsymbol{Q}}$ and $\tilde{\boldsymbol{T}}$ represent the resultant nodal forces, which are obtained from the pressure ($\boldsymbol{P}$), flux ($\boldsymbol{Q}$) and traction ($\boldsymbol{T}$) distributions, respectively. $\boldsymbol{F}$ denotes the FE nodal forces and the negative signs account for the different normal directions on the interface of the coupled sub-domains.

The algorithm shown next summarizes the iterative coupling procedures being used. It is important to note that the iterative coupling process can be done together with the FEM nonlinear iterations, described in section 3.

## Algorithm

### *1. Initial calculations*

1.1 The global domain of the problem is subdivided into different sub-domains; these sub-domains are modeled either by the FEM or the BEM.

1.2 The time-steps for each sub-domain are selected: ${}_F\Delta t$ and ${}_B\Delta t$. The initial time attributions are ${}_Ft = 0$ and ${}_Bt = {}_B\Delta t$.

1.3 Initial prescribed values are chosen for the FEM nodal forces at the interface surfaces, for example, ${}^{I}_{F}\boldsymbol{F}^{F\,\Delta t}_{(0)} = 0$.

1.4 Standard initial calculations related to the FEM and BEM are performed, for instance, the calculation of the matrices $\hat{\boldsymbol{A}}$, $\hat{\boldsymbol{B}}$, etc.

### *2. Time-step loop*

2.1 Beginning of the evaluations at each time-step: ${}_Ft = {}_Ft + {}_F\Delta t$

2.2 BEM pre-iterative processing
If ${}_Ft > {}_Bt$ then: adoption of ${}_Bt = {}_Bt + {}_B\Delta t$; evaluation of $\boldsymbol{S}^{B\,t}$

2.3 Iterative loop

2.3.1 Solve the FEM sub-domain.
*Solid mechanics*: Obtain the displacements ${}^{I}_{F}\boldsymbol{U}^{F\,t}_{(k+\alpha)}$ (*solid-solid coupling*) or the accelerations ${}^{I}_{F}\ddot{\boldsymbol{U}}^{F\,t}_{(k+\alpha)}$ (*fluid-solid coupling*) at the interface.
*Acoustic fluids*: Obtain the hydrodynamic pressures ${}^{I}_{F}\boldsymbol{P}^{F\,t}_{(k+\alpha)}$ at the interface.

2.3.2 Adoption of relaxation parameters to ensure and/or speed up convergence

*Fluid-fluid coupling:* ${}^{I}_{F}\boldsymbol{P}^{F\,t}_{(k+1)} = \alpha\, {}^{I}_{F}\boldsymbol{P}^{F\,t}_{(k+\alpha)} + (1-\alpha)\,{}^{I}_{F}\boldsymbol{P}^{F\,t}_{(k)}$

*Solid-solid coupling:* ${}^{I}_{F}\boldsymbol{U}^{F\,t}_{(k+1)} = \alpha\, {}^{I}_{F}\boldsymbol{U}^{F\,t}_{(k+\alpha)} + (1-\alpha)\,{}^{I}_{F}\boldsymbol{U}^{F\,t}_{(k)}$

*Fluid-solid coupling:* ${}^{I}_{F}\ddot{\boldsymbol{U}}^{F\,t}_{(k+1)} = \alpha\, {}^{I}_{F}\ddot{\boldsymbol{U}}^{F\,t}_{(k+\alpha)} + (1-\alpha)\,{}^{I}_{F}\ddot{\boldsymbol{U}}^{F\,t}_{(k)}$

2.3.3 Obtain the boundary conditions for the BEM sub-domains

*Fluid-fluid coupling:* time extrapolation of ${}^{I}_{F}\boldsymbol{P}^{F\,t}_{(k+1)}$ in order to obtain ${}^{I}_{B}\boldsymbol{P}^{B\,t}_{(k+1)}$. Since the interpolation function $\phi^n(t)$ is usually considered as being linear for hydrodynamic pressures, one has: ${}^{I}_{B}\boldsymbol{P}^{B\,t}_{(k+1)} = ({}^{I}_{F}\boldsymbol{P}^{F\,t}_{(k+1)} - \beta\, {}^{I}_{B}\boldsymbol{P}^{B\,t-{}_B\Delta t}) / (1-\beta)$.

*Solid-solid coupling:* time extrapolation of ${}^{I}_{F}\boldsymbol{U}^{F\,t}_{(k+1)}$ in order to obtain ${}^{I}_{B}\boldsymbol{U}^{B\,t}_{(k+1)}$. Since the interpolation function $\phi^n(t)$ is usually considered as being linear for displacements, one has: ${}^{I}_{B}\boldsymbol{U}^{B\,t}_{(k+1)} = ({}^{I}_{F}\boldsymbol{U}^{F\,t}_{(k+1)} - \beta\, {}^{I}_{B}\boldsymbol{U}^{B\,t-{}_B\Delta t}) / (1-\beta)$.

*Fluid-solid coupling:* from the FEM acceleration ${}^{I}_{F}\ddot{\boldsymbol{U}}^{F\,t}_{(k+1)}$, obtain the BEM flux ${}^{I}_{B}\boldsymbol{Q}^{F\,t}_{(k+1)}$. Use time extrapolation of ${}^{I}_{B}\boldsymbol{Q}^{F\,t}_{(k+1)}$ in order to obtain ${}^{I}_{B}\boldsymbol{Q}^{B\,t}_{(k+1)}$. Since the interpolation function $\phi^n(t)$ is usually considered as being piecewise constant for fluxes, one obtains ${}^{I}_{B}\boldsymbol{Q}^{B\,t}_{(k+1)} = {}^{I}_{B}\boldsymbol{Q}^{F\,t}_{(k+1)}$.

2.3.4 Solve the BEM sub-domain

*Solid mechanics*: obtain the tractions ${}^{I}_{B}\boldsymbol{T}^{B\,t}_{(k+1)}$ at the interface.

*Acoustic fluids*: obtain the fluxes ${}^{I}_{B}\boldsymbol{Q}^{B\,t}_{(k+1)}$ (*fluid-fluid coupling*) or the pressures ${}^{I}_{B}\boldsymbol{P}^{B\,t}_{(k+1)}$ (*fluid-solid coupling*) at the interface.

2.3.5 Determine the boundary conditions for the FEM sub-domain

*Fluid-fluid coupling:* time interpolation of ${}^{I}_{B}\boldsymbol{Q}^{B\,t}_{(k+1)}$ in order to obtain ${}^{I}_{B}\boldsymbol{Q}^{F\,t}_{(k+1)}$. Since the interpolation function $\phi^n(t)$ is usually considered as being piecewise constant for fluxes, one gets ${}^{I}_{B}\boldsymbol{Q}^{F\,t}_{(k+1)} = {}^{I}_{B}\boldsymbol{Q}^{B\,t}_{(k+1)}$. From the BEM fluxes at the interface ${}^{I}_{B}\boldsymbol{Q}^{F\,t}_{(k+1)}$, calculate the FEM nodal forces ${}^{I}_{F}\boldsymbol{F}^{F\,t}_{(k+1)}$.

*Solid-solid coupling:* time interpolation of ${}^{I}_{B}\boldsymbol{T}^{B\,t}_{(k+1)}$ in order to obtain ${}^{I}_{B}\boldsymbol{T}^{F\,t}_{(k+1)}$. Since the interpolation function $\phi^n(t)$ is usually considered as being piecewise constant for tractions, one gets ${}^{I}_{B}\boldsymbol{T}^{F\,t}_{(k+1)} = {}^{I}_{B}\boldsymbol{T}^{B\,t}_{(k+1)}$. From the BEM tractions at the interface ${}^{I}_{B}\boldsymbol{T}^{F\,t}_{(k+1)}$, calculate the FEM nodal forces ${}^{I}_{F}\boldsymbol{F}^{F\,t}_{(k+1)}$.

*Fluid-solid coupling:* time interpolation of ${}^{I}_{B}\boldsymbol{P}^{B\,t}_{(k+1)}$ in order to obtain ${}^{I}_{B}\boldsymbol{P}^{F\,t}_{(k+1)}$. Since the interpolation function $\phi^n(t)$ is usually considered as being linear for hydrodynamic pressures, one gets: ${}^{I}_{B}\boldsymbol{P}^{F\,t}_{(k+1)} = \beta\,{}^{I}_{B}\boldsymbol{P}^{B\,t-{}_{B}\Delta t} + (1-\beta)\,{}^{I}_{B}\boldsymbol{P}^{B\,t}_{(k+1)}$. From the BEM pressures at the interface ${}^{I}_{B}\boldsymbol{P}^{F\,t}_{(k+1)}$, calculate the FEM nodal forces ${}^{I}_{F}\boldsymbol{F}^{F\,t}_{(k+1)}$.

2.3.6 Check for convergence. Go back to 2.3.1 if convergence is not achieved.

2.4 Actualization (and impression) of results related to the FEM.

2.5 If ${}_{F}t + {}_{F}\Delta t > {}_{B}t$ then: actualization (and impression) of results related to the BEM.

2.6 Go back to 2.1 until the final time-step is reached.

### *3. End of calculation*

In the algorithm given above, $\alpha$ stands for the relation parameter, which is further discussed in the next subsection, and $\beta$ is the time interpolation parameter, which is given by $\beta = ({}_{B}t - {}_{F}t)/{}_{B}\Delta t$. As it was previously discussed, in order to take into account different time discretizations for the FEM and the BEM sub-domains, extrapolations and interpolations of the variables related to each numerical approach can be considered. The algorithm presented above shows how this time interpolation/extrapolation procedure should be done, according to the adopted BE formulation (Eq. (16)).

As one can observe, the FE- and the BE-subsystems are solved separately, which means that different solution procedures can be applied to solve the FEM and the BEM system of equations. Thus the symmetry and sparsity of the FEM matrices can easily be taken into account, which results in a more efficient methodology. By solving the FEM and the BEM apart, one also has better-conditioned systems of equations, which is important with respect to the accuracy and effectiveness of the analysis. It should also be pointed out that when a Newton-Raphson procedure is considered, which includes a renewal of the effective stiffness matrix at different iterative steps, the BEM system of equations is not affected by this renewal. In this way a considerable amount of calculations is avoided.

The effectiveness of the iterative coupling methodology is intimately related to the relaxation

parameter selection: an inappropriate selection for $\alpha$ can drastically increase the number of iterations in the analysis or, even worse, make convergence unfeasible. Once appropriate $\alpha$ values are considered, convergence is usually achieved in quite few iterative steps, providing an efficient and robust FEM-BEM coupling technique. In the next sub-section, an expression for an optimal relaxation parameter is deduced.

### *5.1 Optimal relaxation parameter*

In order to evaluate an optimal relaxation parameter, the following square error functional is here minimized

$$f(\alpha) = \left\| {}^{I}_{B}\boldsymbol{V}^{B\,t}_{(k+1)}(\alpha) - {}^{I}_{B}\boldsymbol{V}^{B\,t}_{(k)}(\alpha) \right\|^2 \tag{20}$$

where $\boldsymbol{V}$ stands for displacements, accelerations or hydrodynamic pressures, according to the problem in focus.

Taking into account the relaxation of the selected fields for the $(k+1)$ and $(k)$ iterations, Eqs. 21(a) and (b) may be written, regarding the discussed iterative coupling algorithm.

$${}^{I}_{B}\boldsymbol{V}^{B\,t}_{(k+1)} = \bar{\beta}\,{}^{I}_{F}\boldsymbol{V}^{F\,t}_{(k+1)} + \bar{\boldsymbol{V}} = \bar{\beta}(\alpha_F\,{}^{I}\boldsymbol{V}^{F\,t}_{(k+\alpha)} + (1-\alpha)\,{}^{I}_{F}\boldsymbol{V}^{F\,t}_{(k)}) + \bar{\boldsymbol{V}} \tag{21a}$$

$${}^{I}_{B}\boldsymbol{V}^{B\,t}_{(k)} = \bar{\beta}\,{}^{I}_{F}\boldsymbol{V}^{F\,t}_{(k)} + \bar{\boldsymbol{V}} = \bar{\beta}(\alpha_F\,{}^{I}\boldsymbol{V}^{F\,t}_{(k+\alpha-1)} + (1-\alpha)\,{}^{I}_{F}\boldsymbol{V}^{F\,t}_{(k-1)}) + \bar{\boldsymbol{V}} \tag{21b}$$

where $\bar{\boldsymbol{V}}$ stands for previous time-step contributions and $\bar{\beta}$ represents a time interpolation coefficient.

Substituting Eq. (21) into Eq. (20) yields

$$f(\alpha) = \bar{\beta}^2 \left\| \alpha_F\,{}^{I}\boldsymbol{W}^{F\,t}_{(k+\alpha)} + (1-\alpha)\,{}^{I}_{F}\boldsymbol{W}^{F\,t}_{(k)} \right\|^2 = \tag{22}$$

$$= \bar{\beta}^2(\alpha^2 \left\| {}^{I}_{F}\boldsymbol{W}^{F\,t}_{(k+\alpha)} \right\|^2 + 2\alpha(1-\alpha)({}^{I}_{F}\boldsymbol{W}^{F\,t}_{(k+\alpha)}, {}^{I}_{F}\boldsymbol{W}^{F\,t}_{(k)}) + (1-\alpha)^2 \left\| {}^{I}_{F}\boldsymbol{W}^{F\,t}_{(k)} \right\|^2)$$

where the inner product definition is employed (e.g., $(\boldsymbol{W}, \boldsymbol{W}) = ||\boldsymbol{W}||^2$) and new variables, as defined in Eq. (23), are considered.

$${}^{I}_{F}\boldsymbol{W}^{F\,t}_{(k+\lambda)} = {}^{I}_{F}\boldsymbol{V}^{F\,t}_{(k+\lambda)} - {}^{I}_{F}\boldsymbol{V}^{F\,t}_{(k+\lambda-1)} \tag{23}$$

To find the optimal $\alpha$ that minimizes the functional $f(\alpha)$, Eq. (22) is differentiated with respect to $\alpha$ and the result is set to zero, as described below

$$\alpha \left\| {}^{I}_{F}\boldsymbol{W}^{F\,t}_{(k+\alpha)} \right\|^2 + (1-2\alpha)({}^{I}_{F}\boldsymbol{W}^{F\,t}_{(k+\alpha)}, {}^{I}_{F}\boldsymbol{W}^{F\,t}_{(k)}) + (\alpha-1) \left\| {}^{I}_{F}\boldsymbol{W}^{F\,t}_{(k)} \right\|^2 = 0 \tag{24}$$

Re-arranging the terms in Eq. (24), yields

$$\alpha = ({}^{I}_{F}\boldsymbol{W}^{F\,t}_{(k)}, {}^{I}_{F}\boldsymbol{W}^{F\,t}_{(k)} - {}^{I}_{F}\boldsymbol{W}^{F\,t}_{(k+\alpha)}) \,/\, \left\| {}^{I}_{F}\boldsymbol{W}^{F\,t}_{(k)} - {}^{I}_{F}\boldsymbol{W}^{F\,t}_{(k+\alpha)} \right\|^2 \tag{25}$$

which is an easy to implement expression that provides an optimal value for the relaxation parameter $\alpha$, at each iterative step.

It is important to note that the relation $0 < \alpha \leq 1$ must hold. In the present work, the optimal relaxation parameter is evaluated according to Eq. (25) and if $\alpha \notin (0.01;1.00)$ the previous iterative-step relaxation parameter is adopted. For the first iterative step, $\alpha = 0.5$ is selected.

## 6. Numerical applications

In the next subsections, some numerical applications are presented, illustrating the potentialities and effectiveness of the discussed methodologies. In the first example, fluid-fluid coupling procedures are focused, and a two media model is considered, studding the scalar wave propagation through the different materials. In the second example, solid-solid coupling techniques are discussed, and a circular cavity is analysed, taking into account linear and non-linear behaviour. Finally, in the third application, fluid-solid coupling procedures are employed and a dam-reservoir system is analysed, considering once again linear and non-linear behaviour.

For all the applications that follow, spatial discretization based on linear elements is considered for both BEM and FEM sub-domains. The trapezoidal rule is adopted for time integration, regarding the Newmark method. The convergence of the iterative coupling process is analysed based on the FEM computed fields and residual norms, and a tight tolerance error of $10^{-5}$ is selected. The results obtained with the iterative FEM-BEM coupled formulation are compared with the results from other numerical procedures.

### 6.1 Fluid-fluid coupling

In this application, a fluid-fluid interaction model is analysed taking into account acoustic FEM-BEM coupling procedures. The physical properties of the acoustic fluid modelled by the FEM are $c = 1500\ m/s$ and $\hat{\rho} = 1000\ kg/m^3$; the fluid modelled by the BEM is characterized by $c = 340\ m/s$ and $\hat{\rho} = 1.3\ kg/m^3$. A sketch is depicted in Fig. 1. The geometry of the model is defined by $L = 1.0\ m$ and the FEM and BEM meshes are sufficiently extended horizontally (so that outgoing waves never reach lateral boundaries - uniform meshes with element length $l = 0.1\ m$ are employed). The time-steps considered in the analyses are ${}_B\Delta t = 2 \cdot 10^{-4}\ s$ and ${}_F\Delta t = 1 \cdot 10^{-5}\ s$. One should observe that a great difference between the selected time-step values is being considered. This difference is due to the different wave propagation velocities within the media, requiring very distinct time-steps at each sub-domain, in order to achieve optimal local time discretizations.

The potential time histories at points *A*, *B* and *C*, due to a time-sinusoidal point source, located as

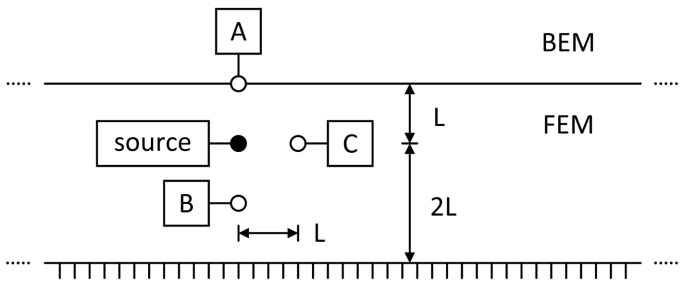


Fig. 1 Sketch of the model for the fluid-fluid interaction analysis

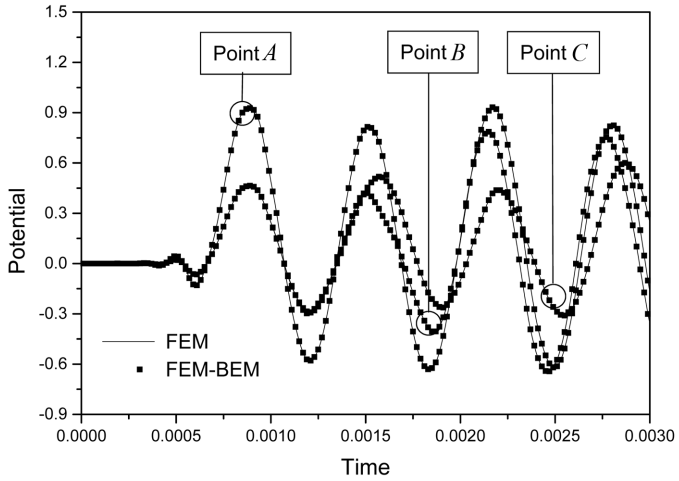


Fig. 2 Time history results at points $A$, $B$ and $C$ for the fluid-fluid interaction analysis

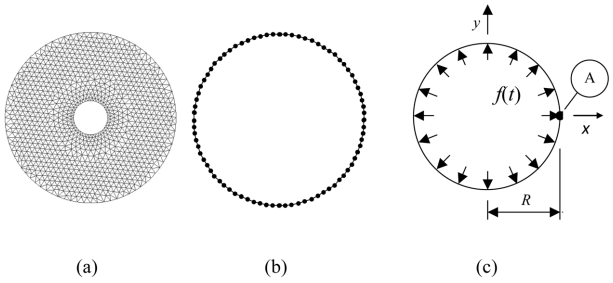


Fig. 3 Circular cavity: (a) FEM mesh, (b) BEM mesh and (c) geometry and boundary conditions

described in Fig. 1, are depicted in Fig. 2. The FEM-BEM results are compared to those provided by FEM analyses based on (vertically) large enough meshes and a unique temporal discretization of $\Delta t = 1 \cdot 10^{-5}\ s$. As can be seen, good agreement between FEM-BEM and FEM results is observed, illustrating the robustness of the adopted time interpolation/extrapolation procedures (it is important to highlight that these procedures are consistent with the boundary element formulations being considered; if different relations are employed for the time interpolation/extrapolation procedures, unstable results usually arise).

### 6.2 Solid-solid coupling

This plane strain problem consists of a circular cavity under a uniform internal pressure ($6.895 \cdot 10^6$ $N/m^2$) suddenly applied and kept constant in time. A sketch of the model is shown in Fig. 3(c). The finite and boundary element meshes are depicted in Figs. 3(a) and (b), respectively: 1944 triangular finite elements and 80 boundary elements are employed in the coupled analysis. The physical properties of the model are: $E = 6.5277 \cdot 10^8\ N/m^2$; $\rho = 1.804 \cdot 10^3\ kg/m^3$ ; $v = 0.2308$. A perfectly plastic material obeying the Mohr-Coulomb yield criterion is assumed, where: $c = 4.8263 \cdot 10^6\ N/m^2$ (cohesion); $\phi = 30^o$ (internal friction angle). The geometry of the problem is defined by $R = 3.048\ m$ (the radius

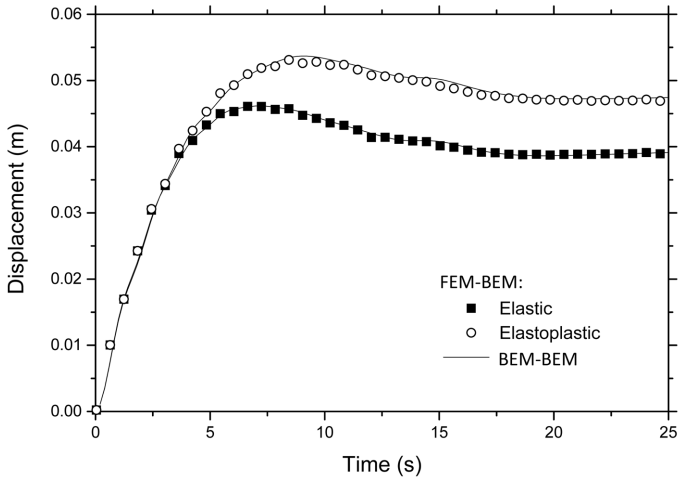


Fig. 4 Horizontal displacements at point $A$ considering elastic and elastoplastic behaviour

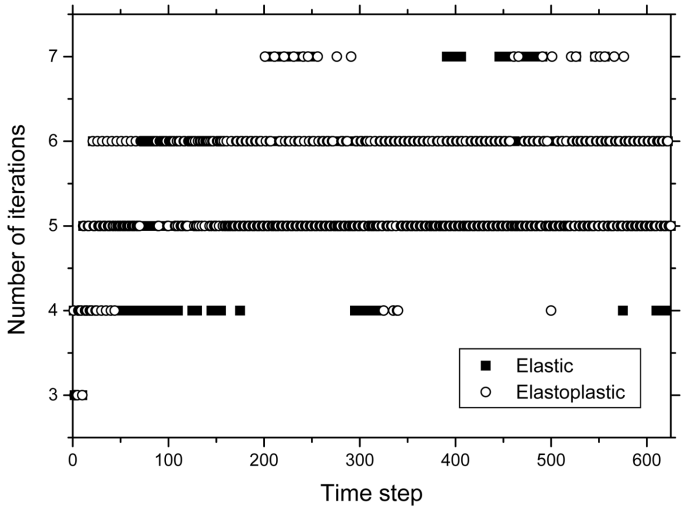


Fig. 5 Number of iterations per time step considering optimal relaxation parameters

of the BEM circular mesh is given by $5R$). The time discretization adopted is given by ${}_F\Delta t = 0.04\ s$ and ${}_B\Delta t = 0.20\ s$.

In Fig. 4, the displacement time history at point $A$ is plotted, considering linear and non-linear analyses (results considering BEM-BEM coupling procedures are plotted for comparison, following the work of Soares *et al*. 2005a). The number of iterations per time-step and the optimal relaxation parameters, evaluated at each iterative step, are plotted in Figs. 5 and 6, respectively. As one may observe, basically the same computational effort is necessary for both linear and non-linear analyses, highlighting the efficiency of the proposed methodology for complex phenomena modeling. For the focused configurations, the optimal relaxation parameters are intricately distributed within the interval (0.75; 1.00), as depicted in Fig. 6.

In Table 1, the total number of iterations is presented, considering analyses with optimal relaxation

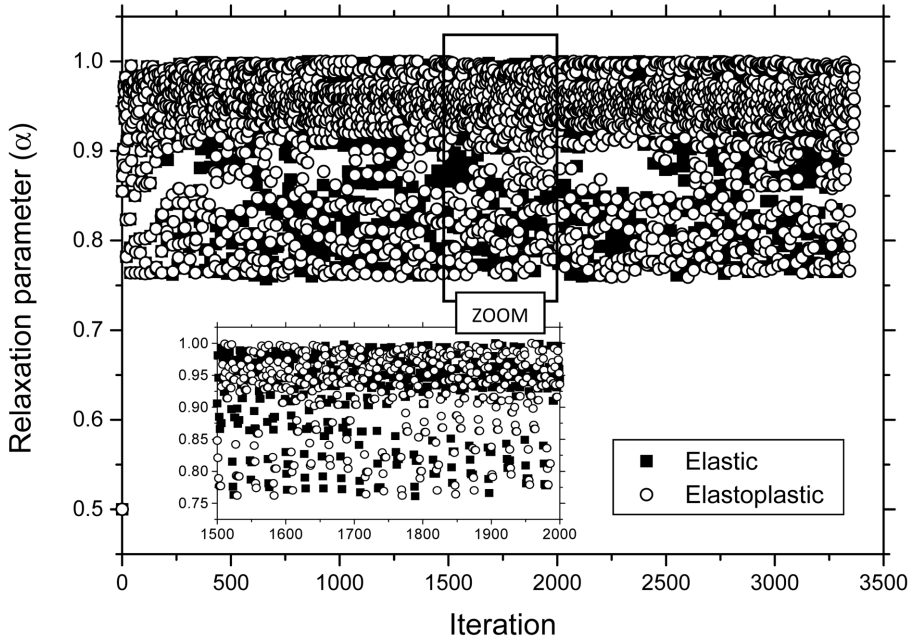


Fig. 6 Optimal relaxation parameters for each iterative step

Table 1 Total number of iterations for the circular cavity analysis

| Relaxation parameter | Elastic analysis | Elastoplastic analysis |
|---|---|---|
| 1.00 | 3730 | 3740 |
| 0.90 | 3392 | 3443 |
| 0.80 | 3973 | 3993 |
| 0.70 | 4772 | 4777 |
| optimal | 3287 | 3346 |

parameters and with some constant pre-selected $\alpha$ values. As one may observe, an inappropriate selection for the relaxation parameter can considerably increase the associated computational effort. Thus, the proposed technique is extremely important in order to provide a robust and efficient iterative coupling formulation.

### 6.3 Fluid-solid coupling

In this second example, a dam-reservoir system, as depicted in Fig. 7, is analysed. The structure is subjected to a sinusoidal distributed vertical load on its crest, acting with an angular frequency $w = 18\ rad/s$ and amplitude $200\ N/m^2$. The material properties of the dam are: $E = 3.437 \cdot 10^9\ N/m^2$, $v = 0.25$ and $\rho = 2000\ kg/m^3$ (a perfectly plastic material obeying the von Mises yield criterion is assumed, with yielding stress $\sigma_0 = 175\ N/m^2$). The adjacent water is characterized by $c = 1436\ m/s$ and $\hat{\rho} = 1000\ kg/m^3$ (a water level defined by H = 50 *m* is considered). 93 quadrilateral finite elements are employed to discretize the dam and the fluid is discretized by constant-length boundary elements ($l = 5\ m$). Regarding temporal discretization, two cases are here considered, namely: (i) case $1 - {}_B\Delta t =$

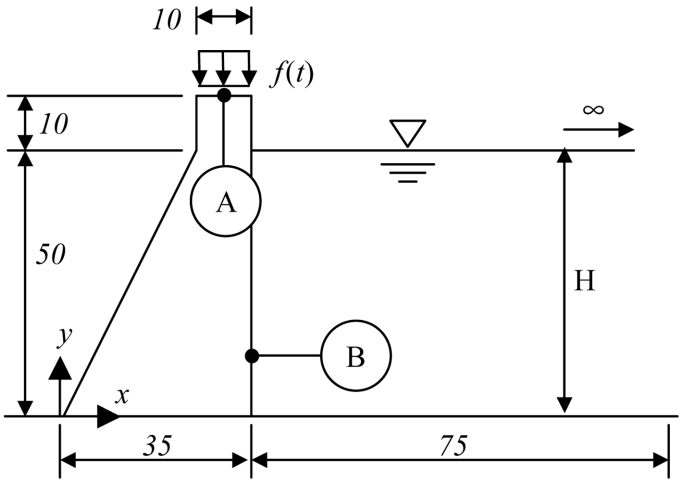


Fig. 7 Dam with a semi-infinite storage-lake: sketch of the model

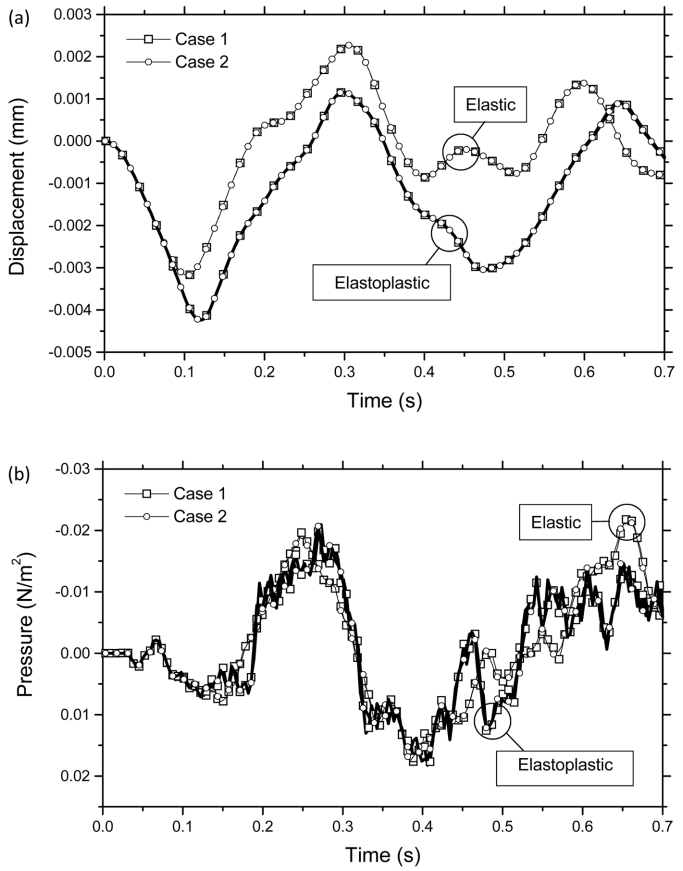


Fig. 8 Time history results considering linear and non-linear material behaviour: (a) vertical displacements at point *A* and (b) hydrodynamic pressures at point *B*

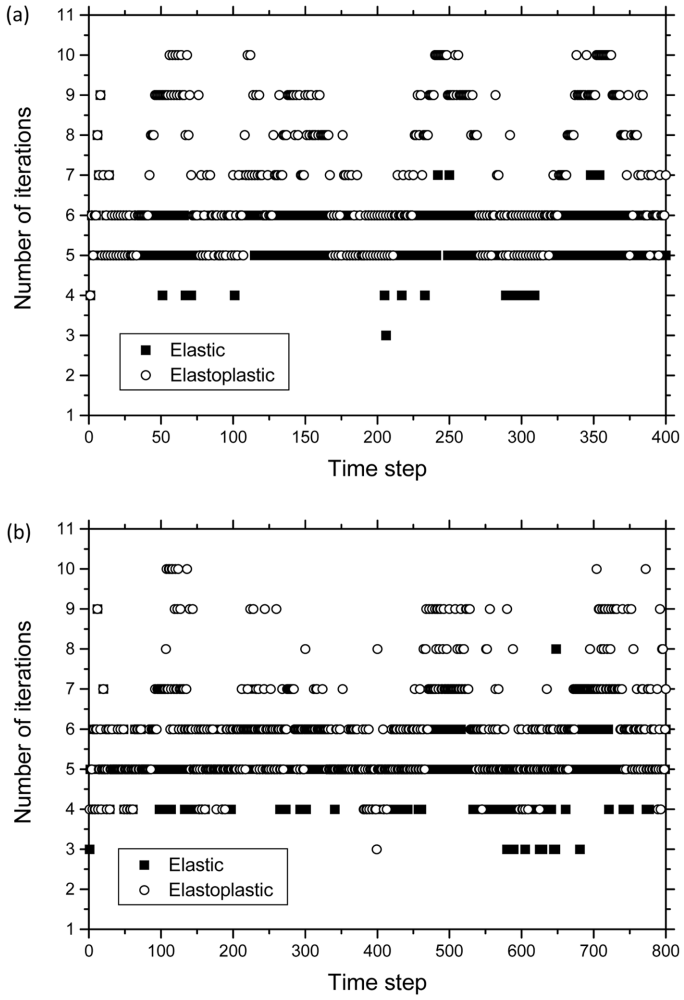


Fig. 9 Number of iterations per time step considering optimal relaxation parameters: (a) case 1 and (b) case 2

0.0035 *s* and ${}_F\Delta t = 0.00175$ *s*; (ii) case 2 – ${}_B\Delta t = 0.0035$ *s* and ${}_F\Delta t = 0.000875$ *s*.

In Fig. 8, vertical displacements at point *A* and hydrodynamic pressures at point *B* are depicted, considering case 1 and case 2, as well as linear and non-linear analyses. In Fig. 9, the number of iterations per time step is presented, considering optimal relaxation parameters (one should keep in mind that a tight tolerance error is being considered). In Fig. 10, the optimal relaxation parameters, evaluated at each iterative step, are plotted. As it can be observed, for the current analyses, the optimal relaxation parameter varies intricately within the interval (0.2;1.0), illustrating the intense dynamic behaviour of this variable along typical fluid-structure interaction analyses.

In Table 2, the total amount of iterations, taking into account non-linear analyses (case 1 and case 2), are specified. The results are presented considering optimal and some constant pre-selected relaxation parameter values. As it can be observed, optimal relaxation parameters reduce the computational cost of the analysis, as well as they ensure convergence in the iterative coupling procedure (in Table 2, the symbol $\infty$ indicates that convergence is not achieved).

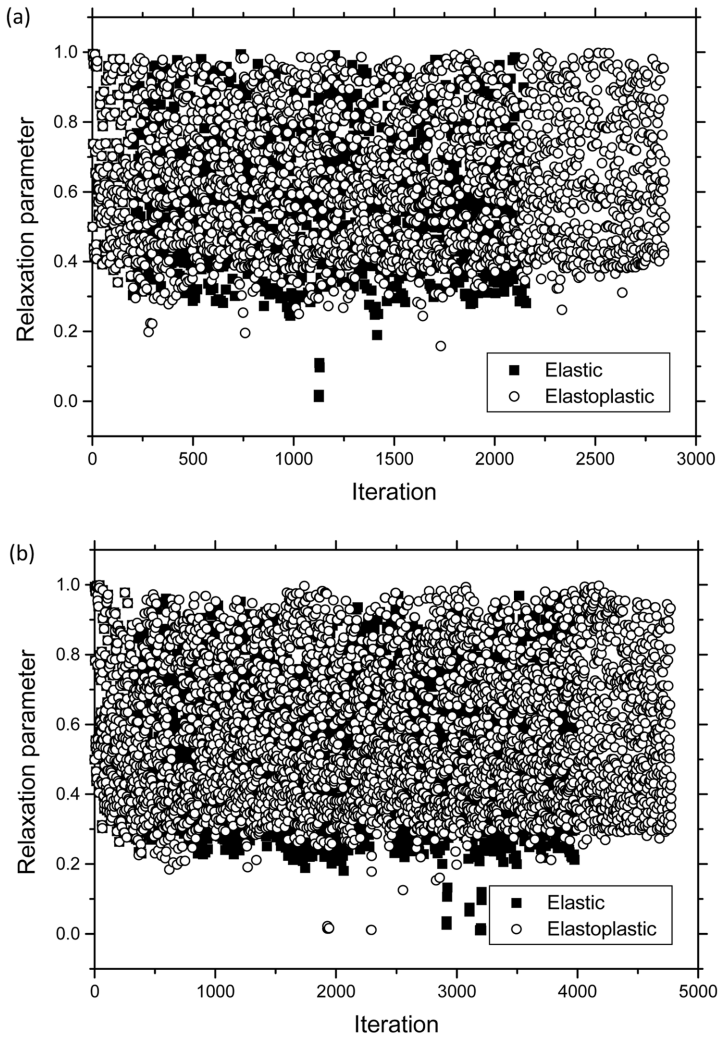


Fig. 10 Optimal relaxation parameters for each iterative step: (a) case 1 and (b) case 2

Table 2 Total number of iterations in the dam-reservoir system non-linear analyses considering different relaxation parameter values

| Relaxation parameter | Case 1 | Case 2 |
|---|---|---|
| 0.3 | 3278 | 4885 |
| 0.6 | 3526 | ∞ |
| 0.9 | ∞ | ∞ |
| optimal | 2825 | 4757 |

## 7. Conclusions

In order to increase the effectiveness of FEM-BEM coupled analyses in the time domain, an iterative

coupling approach has been discussed. It is based on three major steps, namely:
1. subdivision of a given domain problem into a number of sub-domains,
2. modeling of each sub-domain either by finite elements or by boundary elements,
3. iterative coupling of the FEM and BEM sub-domains, taking into account the current transient boundary conditions.

The major advantage of such a procedure can be seen in the fact that the FEM and BEM system matrices are solved separately using optimized solution algorithms for each sub-domain. Consequently, the systems of equations to be solved are much smaller than the standard coupled matrices. In addition, the iterative coupling offers two advantages: It is straightforward to use different time steps in each sub-domain and, moreover, to take into account nonlinearities (within the FEM sub-domains) in the same iteration loop that is needed for the coupling.

The iterative coupling methodology has been applied in three numerical examples, namely considering fluid-fluid, solid-solid and fluid-solid coupling. Assuming linear and also nonlinear material laws, it could be shown that the new algorithm yields excellent results, especially when optimal relaxation parameters are considered, increasing the robustness and efficiency of the methodology. Independent time discretization for each sub-domain of the model also greatly improves the accuracy, stability and versatility of the technique, since it allows more appropriate FEM/BEM local analyses (one should keep in mind that FEM and BEM usually require quite different optimal temporal discretizations, even when homogeneous media are considered; thus, independent temporal discretization for each sub-domain in FEM-BEM coupled analyses of wave propagation models is of major importance).

Using the advantages of finite and boundary elements in an iterative coupling scheme, the discussed formulation is well suited to handle more complex semi-infinite systems including local nonlinearities and highly heterogeneous media. As a matter of fact, the present methodology is very effective to analyze complex wave propagation models, properly jointing "the best of two worlds".

## Acknowledgements

The financial support by CNPq (*Conselho Nacional de Desenvolvimento Científico e Tecnológico*) and FAPEMIG (*Fundação de Amparo à Pesquisa do Estado de Minas Gerais*) is greatly acknowledged.

## References

Bathe, K.J. (1996), *Finite element procedures*, Prentice-Hall.
Becker, A.A. (1992), *The boundary element method in engineering*, McGraw-Hill.
Belytschko, T. and Lu, Y.Y. (1994), "A variational coupled FE-BE method for transient problems", *Int. J. Num. Meth. Eng.*, **37**(1), 91-105.
Belytschko, T., Liu, W.K. and Moran, B (2000), *Nonlinear finite elements for continua & structures*, J. Wiley & Sons.
Beskos, D.E. (1987), "Boundary element methods in dynamic analysis", *App. Mech. Rev.*, **40**(1), 1-23.
Beskos, D.E. (1996), "Boundary element methods in dynamic analysis: Part II", *App. Mech. Rev.*, **50**(3), 149-197.
Beskos, D.E. (2003), *Dynamic Analysis of Structures and Structural Systems*, (Eds. Beskos, D.E. and Maier, G.), Boundary Element Advances in Solid Mechanics, CISM International Centre for Mechanical Sciences, **440**, 1-53.

Crisfield, M.A. (1991), *Non-linear Finite Element Analysis of Solid Structures*, John Wiley & Sons.
Czygan, O. and von Estorff, O. (2002), "Fluid-structure interaction by coupling BEM and nonlinear FEM", *Eng. Anal. Bound. Elem*., **26**(9), 773-779.
Dominguez, J. (1993), *Boundary elements in dynamics*, Computational Mechanics Publications.
Elleithy, W.M., Al-Gahtani, H.J. and El-Gebeily, M. (2001), "Iterative coupling of BE and FE methods in elastostatics", *Eng. Anal. Bound. Elem*., **25**(8), 685-695.
Elleithy, W. and Grzibovskis, R. (2009), "An adaptive domain decomposition coupled finite element - boundary element method for solving problems in elasto-plasticity", *Int. J. Num. Meth. Eng*., **79**, 1019-1040.
Elleithy, W.M. and Tanaka, M. (2002), "BEM-BEM coupling and FEM-BEM coupling via interface relaxation", *Eng. Anal. Bound. Elem*.,**19**(9), 37-42.
Firuziaan, M. and von Estorff, O. (2002), *Transient 3D soil/structure interaction analyses including nonlinear effects*, (Eds. Grundmann, H. and Schuëller, G.I.), Structural Dynamics, EURODYN2002, Swets &Zeitlinger B.V.
Hughes, T.J.R. (1987), *The finite element method*, Prentice-Hall.
Jacob, B.P. and Ebecken, N.F.F. (1994), "An optimized implementation of the Newmark/Newton-Raphson algorithm for the time integration of non-linear problems", *Commun. Numer. Meth. En*., **10**(12), 983-992.
Lin, C.C. (1996), "An iterative finite element-boundary element algorithm", *Comput. Struct*., **59**(5), 899-909.
Mansur W.J. (1983), *A time-stepping technique to solve wave propagation problems using the boundary element method*, Ph.D. Thesis, University of Southampton, England.
Newmark, N.M. (1959), "A method of computation for structural dynamics", *J. Eng. Mech. - ASCE*, **85**(7), 67-94.
Pavlatos, G.D. and Beskos, D.E. (1994), "Dynamic elastoplastic analysis by BEM/FEM", *Eng. Anal. Bound. Elem*., **14**(1), 51-63.
Soares, D. (2008a), "A time-domain FEM-BEM iterative coupling algorithm to numerically model the propagation of electromagnetic waves", *Comput. Model. Eng.Sci*., **32**, 57-68.
Soares, D. (2008b), "An optimised FEM-BEM time-domain iterative coupling algorithm for dynamic analyses", *Comput. Struct*., **86**(19-20), 1839-1844.
Soares, D. (2008c), "Numerical modelling of acoustic-elastodynamic coupled problems by stabilized boundary element techniques", *Comput. Mech*., **42**(6), 787-802.
Soares, D. (2009a), "Acoustic modelling by BEM-FEM coupling procedures taking into account explicit and implicit multi-domain decomposition techniques", *Int. J. Numer. Meth. Eng*., **78**(9), 1076-1093.
Soares, D. (2009b), "An iterative time-domain algorithm for acoustic-elastodynamic coupled analysis considering meshless local Petrov-Galerkin formulations", *Comput. Model. Eng.Sci*., **54**, 201-221.
Soares, D. (2009c), "Fluid-structure interaction analysis by optimised boundary element - finite element coupling procedures", *J. Sound Vib*., **322**(1-2), 184-195.
Soares, D. (2011), *Coupled numerical methods to analyze interacting acoustic-dynamic models by multidomain decomposition techniques*, Mathematical Problems in Engineering, **2011**, 1-28.
Soares, D., Carrer, J.A.M. and Mansur, W.J. (2005a), "Nonlinear elastodynamic analysis by the BEM: an approach based on the iterative coupling of the D-BEM and TD-BEM formulations" *Eng. Anal. Bound. Elem*., **29**, 761-774.
Soares, D., Godinho, L., Pereira, A. and Dors, C. (2012), "Frequency domain analysis of acoustic wave propagation in heterogeneous media considering iterative coupling procedures between the method of fundamental solutions and Kansa's method", *Int. J. Numer. Meth. Eng*., **89**, 914-938.
Soares, D., Mansur, W.J. (2006), "Dynamic analysis of fluid-soil-structure interaction problems by the boundary element method", *J. Comput. Phys*., **219**(2), 498-512.
Soares, D., von Estorff, O. and Mansur, W.J. (2004), "Iterative coupling of BEM and FEM for nonlinear dynamic analyses", *Comput. Mech*., **34**(1), 67-73.
Soares, D., von Estorff, O. and Mansur, W.J. (2005b), "Efficient nonlinear solid-fluid interaction analysis by an iterative BEM/FEM coupling", *Int. J. Numer. Meth. Eng*., **64**(11), 1416-1431.
von Estorff O (Ed.) (2000), *Boundary Elements in Acoustics - Advances and Applications*, WIT Press, Southampton.
von Estorff, O. and Antes, H. (1991) "On FEM-BEM coupling for fluid-structure interaction analysis in the time domain", *Int. J. Numer. Meth. Eng*., **31**(6), 1151-1168.

von Estorff, O. and Firuziaan, M. (2000), "Coupled BEM/FEM approach for nonlinear soil/structure interaction", *Eng. Anal. Bound. Elem*., **24**(10), 715-725.

von Estorff, O. and Hagen, C. (2005), "Iterative coupling of FEM and BEM in 3D transient elastodynamics", *Eng. Anal. Bound. Elem*., **29**(8), 775-787.

von Estorff, O. and Prabucki, M.J. (1990), "Dynamic response in the time domain by coupled boundary and finite elements", *Comput. Mech*., **6**(1), 35-46.

Warszawski, A., Soares, D. and Mansur, W.J. (2008), "A FEM-BEM coupling procedure to model the propagation of interacting acoustic-acoustic / acoustic-elastic waves through axisymmetric media", *Comput. Method. Appl. M*., **197**(45-48), 3828-3835.

Yan B., Du, J. and Hu, N. (2006), "A domain decomposition algorithm with finite element-boundary element coupling", *Appl. Math. Mech - ENGL*., **27**(4), 519-525.

Yazdchi, M., Khalili, N. and Valliappan, S. (1999), "Non-linear seismic behavior of concrete gravity dams using coupled finite element-boundary element technique", *Int. J. Numer. Meth. Eng*., **44**(1), 101-130.

Yu, G., Mansur, W.J., Carrer, J.A.M. and Lie, S.T. (2001), "A more stable scheme for BEM/FEM coupling applied to two-dimensional elastodynamics", *Comput. Struct*., **79**(8), 811-823.

Zienkiewicz, O.C., Kelly D.M. and Bettes, P. (1977), "The coupling of the finite element method and boundary solution procedures", *Int. J. Numer. Meth. Eng*., **11**(2), 355-376.

Zienkiewicz, O.C., Kelly, D.M. and Bettes, P. (1979), *Marriage a la mode - the best of both worlds* (*Finite elements and boundary integrals*), (Eds. Glowinski, R., Rodin, E.Y. and Zienkiewicz, O.C.), Energy Methods in Finite Element Analysis, J. Wiley & Sons.

Zienkiewicz, O.C., and Taylor, R.L. (2002), *The finite element method*, Butterworth-Heinemann, Oxford.